Composite Structures 126 (2015) 62–71

Contents lists available at ScienceDirect

Composite Structures

journal homepage: www.elsevier.com/locate/compstruct

Multiscale model of woven ceramic matrix composites considering manufacturing induced damage

Luke Borkowski *, Aditi Chattopadhyay

School for Engineering of Matter, Transport and Energy, Arizona State University, P.O. Box 876106, Tempe, AZ 85287-6106, United States

ARTICLE INFO

Article history:
Available online 12 February 2015

Keywords:
Ceramic matrix composites
Progressive damage
Micromechanics
Multiscale modeling
Woven composites
Manufacturing-related damage

ABSTRACT

Multiscale models play an important role in capturing the nonlinear response of woven carbon fiber reinforced ceramic matrix composites. In plain weave carbon fiber/silicon carbide (C/SiC) composites, for example, when microcracks form in the as-produced parts due to the mismatch in thermal properties between constituents, a multiscale thermoelastic framework can be used to capture the initial damage state of these composites. In this paper, a micromechanics-based multiscale model coupled with a thermoelastic progressive damage model is developed to simulate the elastic and damage behavior of a plain weave C/SiC composite system under thermal and mechanical loading conditions. The multiscale model is able to accurately predict composite behavior and serves as a valuable tool in investigating the physics of damage initiation and progression, in addition to the evolution of effective composite elastic moduli caused by temperature change and damage. The matrix damage initiation and progression is investigated at various length scales and the effects are demonstrated on the global composite behavior.

1. Introduction

The extreme stiffness, strength, and toughness, as well as nonbrittle failure of advanced ceramic matrix composites (CMCs) make them an ideal choice over monolithic ceramics for many aerospace applications, such as hot engine components [11,22,6,8,12,2,9]. Ceramic matrix composites also offer oxidation and creep resistance, as well as thermal shock stability at elevated temperatures. However, under extreme loading and environmental conditions, the structural reliability of these composites remains a critical issue because a damage event will compromise the integrity of the composite structure, resulting in ultimate failure. Damage in CMCs can initiate at the fiber, matrix, tow, or weave levels. The widespread use of CMCs in critical aerospace components such as turbine blades and thermal barriers, therefore, necessitates development of physics-based models that accurately account for constitutive linear elastic and nonlinear behavior at the pertinent length scales of these materials. Multiscale models can link constitutive model parameters and behavior at the micro- and mesoscale to damage evolution at the macroscale, thus further extending our understanding of damage initiation and propagation in heterogeneous material systems. Traditional analysis methods for composites account for only macroscopic or structural level responses, rendering them inadequate in capturing the complex multiscale phenomena governing composite behavior. Multiscale physics-based models, on the other hand, are well suited for structural analysis because they can effectively determine stress, strain, stiffness, damage, and various state variables at multiple length scales. These models also enable information transfer between scales using appropriate localization and homogenization techniques.

In this work, a recently developed multiscale modeling technique is further extended to incorporate manufacturing-related, temperature-dependent damage behavior as a function of thermal and mechanical loading and nonuniform void distribution in CMCs. The Multiscale Generalized Method of Cells (MS-GMC), developed by Liu et al. [16] extends the Generalized Method of Cells (GMC) theory [23,1] to include additional length scales beyond the micro- and global scales, therefore allowing for the analysis of woven or braided composites. Hence, the number of length scales under investigation is not limited by the analysis technique, but rather can be determined by the physically relevant length scale dependent phenomena that must be captured in the analysis. For example, in the case of a woven composite, as shown in Fig. 1, the relevant length scales may include: (i) constituent level (microscale), (ii) tow level (mesoscale), (iii) weave level (macroscale), and (iv) structural level. Fig. 1 also demonstrates the relevant features at each length scale taken into consideration in the multiscale

* Corresponding author.
E-mail addresses: Luke.Borkowski@asu.edu (L. Borkowski), aditi@asu.edu (A. Chattopadhyay).

http://dx.doi.org/10.1016/j.compstruct.2015.02.015
0263-8223/

analysis, including the void structure within the inter- and intratow matrix.

The MS-GMC framework used in this work has previously been demonstrated effective for predicting the linear elastic and nonlinear behavior of different types of composites (e.g., polymer and ceramic matrix composites with woven and braided architectures) in a highly computationally efficient manner [16,17,18]. This framework is further extended to include the following important manufacturing related phenomena in CMCs: (i) thermal residual stress and damage state following manufacturing; (ii) interaction between nonuniform void distributions and stress and damage fields; and (iii) global nonlinear behavior due to multiscale damage and release of thermal residual stresses.

The material system analyzed in this article is a carbon fiber reinforced, silicon carbide matrix (C/SiC), plain weave composite. The triply periodic plain weave repeating unit cell (RUC) analyzed using the MS-GMC framework is assumed to be representative of the entire periodic composite structure. For the analysis, the weave is discretized into several sub-volume cells, as seen in Fig. 2. In this figure, the through-thickness discretization utilized by MS-GMC to represent the woven tow architecture is evident; the four cells in the thickness direction are composed of either matrix subcells (red) or tow subcells (white with black lines representing tow fiber direction). The specific CMC under investigation is manufactured through densification of the carbon fiber preform via a chemical vapor infiltration (CVI) process, which follows the coating of the carbon fibers with a pyrolytic carbon (PyC) interphase, also performed via CVI [12]. Since the carbon fibers are susceptible to corrosion at elevated temperatures, the PyC interphase offers increased corrosion resistance while also serving as a toughing mechanism through crack deflection, fiber/matrix debonding, and fiber pullout [14]. Due to the manufacturing process and insufficient infiltration (i.e., canning) of the matrix material, voids are distributed in the composite nonuniformly [29]. Using the MS-GMC multiscale modeling scheme, the effects of void localization, volume fraction, and shape on the nonlinear damage-driven macroscopic CMC response were previously investigated in a deterministic and stochastic framework by Liu and Arnold [17] and Liu and Arnold [18], respectively. It was concluded that void physical parameters, especially shape and localization, greatly influence the elastic and damage characteristics of a CMC. The nonuniform shape and size of voids in the composite microstructure is considered in the analyses presented in this article and described in further detail in Section 2.1.

The innovative aspect of this research lies in the inclusion of manufacturing process effects within the multiscale analysis on the as-produced state and nonlinear mechanical behavior of the

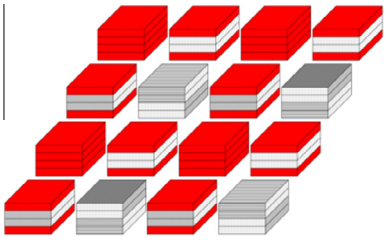

Fig. 2. Plain weave RUC with localized void structure.

composite under mechanical and thermal loading conditions and in the presence of nonuniform and multiscale void structure. The CVI process, which is typically isothermal and isobaric and is carried out at a temperature between 900 °C and 1100 °C [21], is examined. As the specimen cools to room temperature following CVI, the mismatch in the temperature-dependent coefficients of thermal expansion (CTEs) between the carbon fiber and silicon carbide matrix, as presented in Figs. 3 and 4, respectively, causes thermal residual stresses to develop in the composite. Specifically, large residual stresses develop between the plies of the laminated composite and at the fiber/matrix interface during the cool-down phase following manufacturing. The residual stresses, in turn, cause microcracks to form in the inter- and intratow matrix. Because of the heterogeneity and architecture of the woven composite material system, the manufacturing-induced damage is distributed nonuniformly within the composite. Accounting for the presence, distribution, and severity of such damage in the

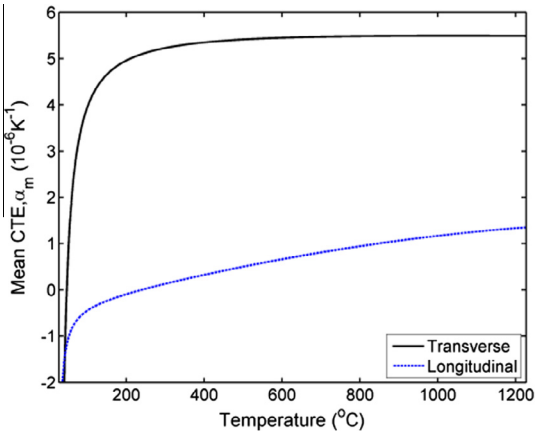

Fig. 3. Carbon fiber CTE vs. temperature [26].

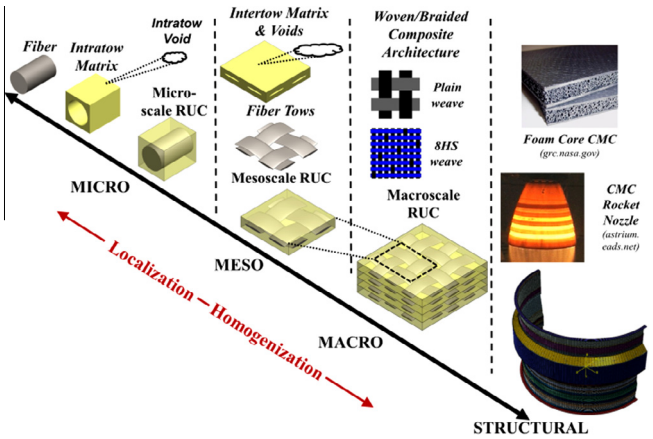

Fig. 1. Concurrent multiscale model analysis framework.

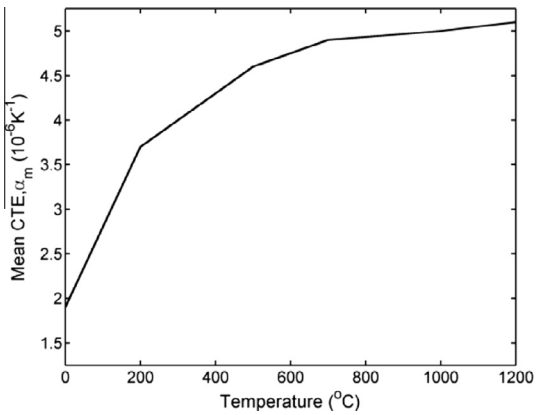

Fig. 4. Matrix CTE vs. temperature [7].

as-produced state of the composite is critical for predicting the as-received mechanical properties, further damage evolution and progression, and subsequent failure in CMC structural components. This research contributes to the core focus of the Integrated Computational Materials Engineering (ICME) approach which aims to integrate the length and time scales, processing/manufacturing conditions, structural and architectural information, and constituent behavior of materials into a comprehensive, multiscale modeling scheme for the purpose of improving material design and optimization [24].

In woven CMCs manufactured through the CVI process, the complex damage behavior is due in part to tow undulation and crossing, porous intratow matrix, and large intertow voids [25,13,11,3]. Addressing this problem with a multiscale framework allows for the damage to be captured at the most relevant length scale (i.e., matrix constituent level). Additionally, a continuum damage mechanics based progressive damage model is developed, and damage evolution is tracked across the length scales using state variables. The progressive damage approach allows for subcells to continue carrying load even after the initiation of damage, as opposed to other approaches that utilize maximum stress/strain or failure laws (e.g., [22,9]. In addition, the presence of nonuniform void shape and size affects the global moduli and damage behavior of the composite. The presence of severe matrix microcracking in the as-produced C/SiC composite [29] results in the material system exhibiting nonlinearity in its mechanical behavior, even at very low stress levels. Therefore, in addition to stimulating thermally induced damage, the multiscale model developed in this work will also be able to predict the nonlinear behavior of the composite when subsequent mechanical loading is applied.

2. Modeling ceramic woven composites

2.1. Void and interphase modeling

In CMCs manufactured via the CVI process, the concentration of voids in the weave tends to be nonuniform due to insufficient and uneven infiltration of the matrix material into the carbon fiber preform [29]. Optical micrographs, such as those presented in Sullivan et al. [29] and Murthy et al. [22] demonstrate the variation in void shape, size, and distribution as a function of location within the composite. Typically, the intertow matrix surrounding the regions in which a tow is undulating has a higher volume fraction of voids compared with those away from the regions of undulation. Additionally, these voids tend to be sheet-like in form. Therefore, the model accounts for this variation in intertow matrix void distribution, size, and shape as a mesoscale input parameter. Voids also exist within the intratow matrix cells and micrographs indicate that these voids are evenly dispersed and approximately equal in size [29,22,6,8]. The meso- and microscale voids are accounted for at a length scale below that of the tow or constituent level, depending on the location of the void, by analyzing a separate RUC and homogenizing the properties to provide higher length scale effective properties [17]. The purpose of analyzing a separate RUC for the void subcells is twofold: (i) to dampen the effects the voids have on the stiffness reduction of the row and column in which the void resides within the RUC and (ii) to represent the voids in a more accurate and generalized framework. In GMC theory, because of the constant strain field assumption within a subcell, a subcell with an approximate zero stiffness (e.g., a void subcell) will cause the entire row and column in which it resides within the RUC to be eliminated due to homogenization [30].

The fiber tow bundles are modeled as a 4×4 doubly periodic RUC, as presented in Fig. 5(a), consisting of a fiber cell (black), the surrounding interphase material cells (shaded), and the intratow matrix cells (red). The intra- and intertow voids are accounted for by modeling the matrix cells containing the voids as $2 \times 2 \times 2$ subcells consisting of one cube-like void cell (white) and seven matrix subcells (red) as seen Fig. 5(b) and as 4×1 subcells consisting of one sheet-like void cell (white) and three matrix subcells (red) as seen Fig. 5(c), respectively. The size of the void cell is a function of the void volume fraction. The scale at which the subcells containing voids is modeled (meso- or microscale) depends on the location of the matrix subcell (within or between fiber tow bundles). Modeling the voids and fiber interphase as described provides a generalized framework in which to model the meso- and microscale architecture and material properties of a CMC composite while capturing the effect of voids on the composite behavior as a result of stress concentrations, reduction in effective elastic properties, and damage initiation and propagation.

2.2. Constitutive relations and damage model

Due to the nature of CMCs (e.g., high void content, weak fiber/matrix bonding, quasi-brittle matrix), multiscale models have the potential to play a key role in predicting the initiation and progression of damage at the most relevant scale, while propagating this information, using homogenization and localization approaches, to the length scales of greatest interest. Liu and Arnold [17] have developed a damage mechanics-based progressive damage model for the ceramic constituent material in CMCs. This damage model is extended to also include thermal coupling and temperature dependent material properties and model parameters. Matrix damage initiation and propagation in the model is represented by a scalar damage mechanics constitutive model, which is driven by the magnitude of the hydrostatic stress and strain tensor. Damage criteria based on the magnitude of the hydrostatic strain tensor have previously been utilized successfully to represent the damage behavior of quasi-brittle matrix material systems [20,27,15]. Aboudi [2] utilized the anisotropic damage law, proposed by Lemaitre and Desmorat [15], and coupled it with the High Fidelity Generalized Method of Cells (HFGMC) micromechanics framework to predict the damage evolution in ductile and quasi-brittle matrix composites. Wu et al. [31] demonstrated that for composite systems with quasi-brittle matrices loaded in tension, fracture is predominately activated by tensile damage mechanisms in both the deviatoric and volumetric stress spaces. In other words, mode I fracture is the dominant failure mode in these systems [27,31].

Damage initiation and progression in the developed model is governed by a bilinear constitutive relation for the elastic/damageable matrix subcells where the model parameters n and σ_{crit} represent the damage normalized secant modulus and the critical stress at which damage initiates, respectively. The

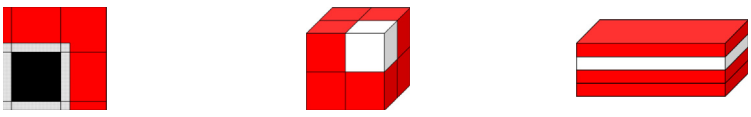

(a) 4x4 fiber tow bundle RUC (b) 2x2x2 intratow matrix RUC (c) 4x1 intertow matrix RUC

Fig. 5. RUCs employed at the micro- and mesoscales to account for matrix void architectural variability.

application of the damage law at the microscale matrix constituent level permits the use of such a model since the dilation at the material point will serve to separate the material particles, thereby initiating a matrix microcrack. The material properties (e.g., K^0), model parameters (e.g., n and σ_{crit}), and stress and strain are assumed to be functions of temperature to allow for the consideration of thermal effects on the constitutive and damage behavior of the composite. Although the present damage law is isotropic at the matrix subcell level, the aggregate effect of each individual subcell on the behavior at the higher length scales can be, in fact, highly anisotropic, depending on the loading and boundary conditions imposed.

The CMC constituent, silicon carbide (SiC), is modeled as a homogeneous, isotropic material with temperature-dependent properties subjected to the proposed scalar progressive damage law. The equivalent stress and strain in the matrix material, denoted by subscript '*eq*', are functions of the undamaged temperature-dependent material bulk modulus and coefficient of thermal expansion (i.e., K^0 and α^0 respectively) and the relative change in temperature, ΔT. Damage initiates in the material subcell once the equivalent stress reaches a critical value for the particular material (σ_{crit}). As seen in Eq. (1), the critical equivalent stress can be a function of strain rate and temperature.

$$\sigma_{eq}\left(\varepsilon_{eq}, \Delta T, K^0, \alpha^0\right) \geqslant \sigma_{crit}(\dot{\varepsilon}, T) \tag{1}$$

Once the critical stress value in a matrix cell is exceeded, a scalar damage parameter, ϕ, accounts for the progressive microcracking that occurs in the matrix as a result of thermal and mechanical loading. Therefore, ϕ scales the elastic stiffness tensor and ranges from zero (i.e., undamaged) to one (i.e., complete loss of load carrying capacity). The multiscale micromechanics-based modeling framework allows the progressive damage to be accounted for with a scalar quantity since the composite is modeled at the individual constituent level, therefore capturing the damage at the most relevant length scale. Additionally, the damage scalar at the constituent level can be homogenized and propagated up the length scales as a state variable, providing the effect of the microscale damage at each length scale considered in the analysis. The scalar damage parameter is incorporated into the matrix temperature-dependent constitutive relation yielding a thermoelastic damage constitutive relation, as seen in Eq. (2). In Eq. (2), the elastic strain ($\boldsymbol{\varepsilon}^e$) is expressed as the total strain ($\boldsymbol{\varepsilon}$) minus the thermal strain ($\boldsymbol{\varepsilon}^t = \boldsymbol{\alpha}\Delta T$) using classical additive decomposition of strain. Accounting for the thermal strains in this analysis permits consideration of the damage and mechanical effect on the composite caused by the CTE mismatch between the constituent materials.

$$\boldsymbol{\sigma} = (1-\phi)\mathbf{C}(\boldsymbol{\varepsilon} - \boldsymbol{\alpha}\Delta T) = (1-\phi)\mathbf{C}\boldsymbol{\varepsilon}^e \tag{2}$$

where $\boldsymbol{\sigma}$ is the second-order Cauchy stress tensor and $\mathbf{C}$ is the fourth-order linear elastic stiffness tensor.

A damage rule based on the theory of elasticity in differential form is defined, as in Eq. (3) where the equivalent stress and strain are defined as the hydrostatic stress and strain respectively, to govern the magnitude/progression of damage:

$$f = 3nK^0(T)\delta\varepsilon^e_{eq} - \delta\sigma_{eq} = 0 \tag{3}$$

where n represents the damaged normalized secant modulus; K^0 is the undamaged tangent bulk modulus as a function of temperature; and

$$\delta\varepsilon^e_{eq} = \left(\delta\varepsilon_{eq} - \delta\alpha^0(T)\Delta T - \alpha^0(T)\delta\Delta T\right) \tag{4}$$

provides the elastic portion of the increment in the strain tensor. $\delta\varepsilon_{eq}$ is the increment in the total equivalent strain tensor, and

$$\delta\sigma_{eq} = 3K(\lambda, K^0)\delta\varepsilon^e_{eq} \tag{5}$$

where $\lambda = (1-\phi)$. The damage rule can be expressed in incremental form as

$$f = 3nK^0(T^{n+1})\delta\varepsilon^{e,n+1}_{eq} - \delta\sigma^{n+1}_{eq} = 0 \tag{6}$$

where T^{n+1} is the temperature at the next increment and $\delta\varepsilon^{e,n+1}_{eq}$ and $\delta\sigma^{n+1}_{eq}$ are the increments in elastic strain and stress tensors, respectively.

In order to derive an expression for $\delta\sigma^{n+1}_{eq}$ in terms of the temperature-dependent undamaged bulk modulus, the expressions for σ^{n+1}_{eq} and σ^{n}_{eq} are expressed as

$$\sigma^{n+1}_{eq} = 3n\Big(K^0(T^n) + \delta K^0(T^{n+1})\Big)\Big[\Big(\varepsilon^n_{eq} + \delta\varepsilon^{n+1}_{eq}\Big) - \Big(\alpha^0(T^n) + \delta\alpha^0(T^{n+1})\Big)\Big(\Delta T^n + \delta\Delta T^{n+1}\Big)\Big] \tag{7}$$

and

$$\sigma^n_{eq} = 3nK^0(T^n)\Big[\varepsilon^n_{eq} - \alpha^0(T^n)\Delta T^n\Big] \tag{8}$$

By subtracting Eq. (8) from (7) and ignoring higher order terms, we obtain the expression for the increment in equivalent stress as a function of the undamaged bulk modulus, Eq. (9).

$$\delta\sigma^{n+1}_{eq} = 3n\Big\{K^0(T^n)\Big[\delta\varepsilon^{n+1}_{eq} - \alpha^0(T^n)\delta\Delta T^{n+1} - \delta\alpha^0(T^{n+1})\Delta T^n\Big] + \delta K^0(T^{n+1})\Big[\varepsilon^n_{eq} - \alpha^0(T^n)\Delta T^n\Big]\Big\} \tag{9}$$

Expanding the second term in the damage law as a function of the instantaneous bulk modulus requires casting the increment in stress in terms of strain as follows:

$$\sigma^{n+1}_{eq} = 3\Big[\Big(\varepsilon^n_{eq} + \delta\varepsilon^{n+1}_{eq}\Big) - \Big(\alpha^0(T^n) + \delta\alpha^0(T^{n+1})\Big)\Big(\Delta T^n + \delta\Delta T^{n+1}\Big)\Big] \tag{10}$$

$$\sigma^n_{eq} = 3K^n\Big(\varepsilon^n_{eq} - \alpha^0(T^n)\Delta T^n\Big) \tag{11}$$

and subtracting Eq. (11) from Eq. (10), we obtain

$$\delta\sigma^{n+1}_{eq} = 3\Big[K^n\Big(\delta\varepsilon^{n+1}_{eq} - \alpha^0(T^n)\delta\Delta T^{n+1} - \delta\alpha^0(T^{n+1})\Delta T^n\Big) + \delta K^{n+1}\Big(\varepsilon^n_{eq} - \alpha^0(T^n)\Delta T^n\Big)\Big] \tag{12}$$

where the instantaneous bulk modulus at the current and next increment, K^n and K^{n+1}, respectively, are expressed in terms of the original, undamaged bulk modulus, the current damage scalar, and the increment in the damage scalar as seen in Eqs. (13) and (14), recalling that $\lambda = (1-\phi)$.

$$K^n = \lambda^n K^0(T^n) \tag{13}$$

$$K^{n+1} = (\lambda^n + \delta\lambda^{n+1})\Big(K^0(T^n) + \delta K^0(T^{n+1})\Big) \tag{14}$$

The increment in the instantaneous bulk modulus is obtained through subtraction of Eq. (13) from Eq. (14), resulting in the following expression after ignoring all higher order terms.

$$\delta K^{n+1} = \lambda^n\delta K^0(T^{n+1}) + \delta\lambda^{n+1}K^0(T^n) \tag{15}$$

After substituting the derived expressions for the terms in the damage rule, we obtain

$$f = n\Big[\delta K^0(T^{n+1})\varepsilon^n_{eq} - \delta K^0(T^{n+1})\alpha^0(T^n)\Delta T^n + K^0(T^n)\delta\varepsilon^{n+1}_{eq} - K^0(T^n)\alpha^0(T^n)\delta\Delta T^{n+1} - K^0(T^n)\delta\alpha^0(T^{n+1})\Delta T^n\Big] - \Big[K^n\Big(\delta\varepsilon^{n+1}_{eq} - \alpha^0(T^n)\delta\Delta T^{n+1} - \delta\alpha^0(T^{n+1})\Delta T^n\Big) + \delta K^{n+1}(\varepsilon^n_{eq} - \alpha^0(T^n)\Delta T^n)\Big] = 0 \tag{16}$$

Following simplification and collection of like terms, solving for the increment in one minus the damage scalar (i.e., $\delta\lambda^{n+1}$) yields the formulation for the incremental, temperature-dependent, thermoelastic progressive damage law.

$$\delta\lambda^{n+1} = \frac{\left(n\left[\delta K^0(T^{n+1})\left(\varepsilon_{eq}^n - \alpha^0(T^n)\Delta T^n\right) + K^0(T^n)\left(\delta\varepsilon_{eq}^{n+1} - \alpha^0(T^n)\delta\Delta T^{n+1} - \delta\alpha^0(T^{n+1})\Delta T^n\right)\right]\right.}{\left.-\lambda^n\left\{K^0(T^n)\left(\delta\varepsilon_{eq}^{n+1} - \alpha^0(T^n)\delta\Delta T^{n+1} - \delta\alpha^0(T^{n+1})\Delta T^n\right) + \delta K^0(T^{n+1})\left(\varepsilon_{eq}^n - \alpha^0(T^n)\Delta T^n\right)\right\}\right)}{K^0(T^n)\left(\varepsilon_{eq}^n - \alpha^0(T^n)\Delta T^n\right)} \tag{17}$$

The T300 carbon fibers of the plain weave preform used as reinforcement in the CMC material system under investigation behave linear elastically and fail under the Hashin failure criterion [10,4]. This criterion applied within the multiscale framework determines the catastrophic/brittle failure of each individual carbon fiber and is based on the axial and shear strengths of the fiber material, as seen in Eq. (18). Once the failure criterion exceeds a value of unity, the stiffness of the fiber is reduced to zero, thus redistributing the load away from the failed fiber and to the surrounding fibers and matrix. The compliant pyrolytic carbon interphase applied to the fibers during the CVI manufacturing process is assumed to fail with the fiber and does not contribute to the transverse failure modes because of its relatively low stiffness.

$$h = \frac{\sigma_{11}^2}{\sigma_{axial}^2} + \frac{1}{\tau_{axial}^2}\left(\sigma_{13}^2 + \sigma_{12}^2\right) \tag{18}$$

2.3. Physical model architectural and mechanical properties

The weave and tow architectural properties for the composite material system under investigation are presented in Tables 1 and 2, respectively. The T300 carbon fibers are modeled as transversely isotropic and the CVI-SiC and CVI-PyC as isotropic materials. The elastic constants for the T300 carbon fiber and PyC interphase do not vary significantly with temperature and therefore were assumed constant as seen in Table 3. However, the CTEs for these two materials were considered as functions of temperature. The temperature-dependent axial and transverse CTEs for the carbon fiber from Pradere and Sauder [26] are presented in Fig. 3. Luo and Cheng [19] provided the tabular CTE data for the PyC interphase material (Fig. 6). The isotropic CTE and tensile modulus for the CVI-SiC (Figs. 4 and 7, respectively) were adapted from Dow Chemical Company [7]. The spatial variation of thermal properties due to architectural and constituent variability causes the development of thermal strains, which in turn contribute to the microcracks and residual stresses present in the as-produced composite.

Table 1
C/SiC weave architecture properties.

Type	Plain
Total fiber volume fraction	43%
Total void volume fraction	15.3%
Weave void volume fraction	10%, 80%
Total thickness	6.55 mm
Matrix	CVI-SiC
Interphase	PyC

Table 2
Plain weave C/SiC tow architecture properties.

Tow fiber volume fraction	56%
Tow void volume fraction	3%
Tow packing structure	Square
Fiber	T300 carbon
Matrix	CVI-SiC
Interphase	PyC

Table 3
Constituent material properties.

Constituent	T300	CVI-PyC
E_{11} (GPa)	231.0	20
E_{22} (GPa)	22.4	20
G_{12} (GPa)	15.0	8.13
ν_{12}	0.3	0.23
ν_{23}	0.35	0.23

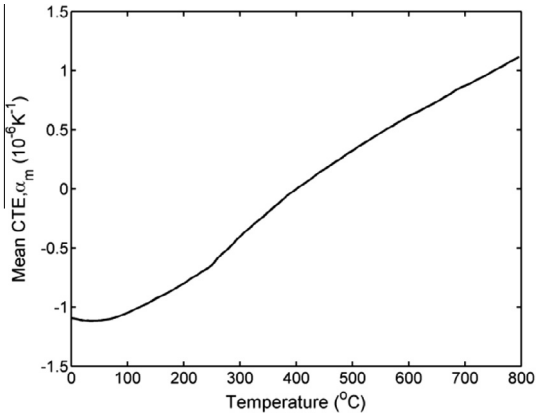

Fig. 6. PyC CTE vs. temperature [19].

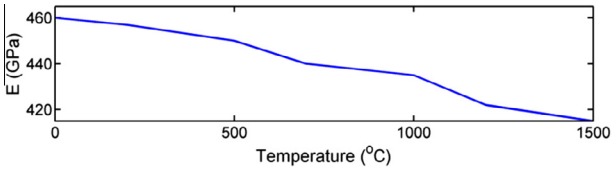

Fig. 7. Matrix tensile modulus vs. temperature [7].

3. Results and discussion

The thermal constitutive model and homogenization of the constituent level CTEs to the macroscale using the MS-GMC framework utilized in this paper was validated by simulating the global longitudinal and transverse CTE of a unidirectional polymer

Table 4
Fiber properties [5].

Fiber	E_{11} (GPa)	E_{22} (GPa)	G_{12} (GPa)	G_{23} (GPa)	ν_{12}	ν_{23}	(10^{-6}/°C)	
							α_1	α_2
T300	233.0	23.1	9.0	8.3	0.20	0.40	−0.54	10.08
HMS	379.2	6.2	7.6	2.2	0.20	0.40	−0.99	6.84

Table 5
Matrix properties [5].

Matrix	E (GPa)	G (GPa)	ν	α (10^{-6}/°C)
934 epoxy	4.3	1.6	0.37	43.92
Borosilicate glass	62.7	26.2	0.20	3.24

matrix composite (T300/934) with a 57% fiber volume fraction and a ceramic matrix composite (HMS/Borosilicate) with a fiber volume fraction of 47%, and comparing these results to those obtained using a high-fidelity finite element model from Bowles and Tompkins [5]. The transversely isotropic fiber and isotropic matrix constituent material properties for the two validation models are presented in Tables 4 and 5, respectively. The results from the multiscale thermal model, presented in Table 6, were within ∼5% of the finite element results. Once the thermal composite behavior was validated, the plain weave carbon fiber reinforced CMC detailed in Tables 1–3 was used to validate the developed thermoelastic constitutive relation with progressive matrix damage for thermal and mechanical loading. Damage model parameters values of 180 MPa and 0.04 were used for the critical stress (σ_{crit}) and the damage normalized secant modulus (n), respectively [17]. The composite was subjected to a two-part loading scheme that involved a globally stress-free cool-down from the manufacturing temperature of ∼1000 °C to room temperature, followed by the loading of the specimen in uniaxial strain. During cool-down, the temperature was incremented by 1 °C for a total temperature change of 1000 °C to ensure convergence. It is assumed that the slow rate of passive cooling does not induce significant thermal gradients. Due to a mismatch in CTE between the fiber and matrix materials, damage occurred during the cool-down phase, thereby introducing microcracks that reduce the initial modulus of the as-produced composite and leave the composite in a prestressed state. Following cool-down, loading the specimen in tension caused the damage to progress further, contributing to the nonlinear tensile behavior of the C/SiC composite. The results from the simulation were compared to the experimental results from Jacobsen and Brøndsted [12], as seen in Fig. 8. To determine if the as-produced mechanical state of the composite was accurately predicted, the initial tensile modulus was compared to experimental data from Jacobsen and Brøndsted [12] and Shuler et al. [28]. The initial tensile modulus is taken as the slope of the uniaxial tensile stress/strain curve before 'yielding' or further damage occurs (i.e., kink in the stress/strain response). The initial tensile modulus obtained from the thermoelastic simulation was

Table 6
Prediction of global composite CTE.

	Present model	FEM
T300/934 (PMC)		
α_l	0.084e−6/°F	0.089e−6/°F
α_t	16.56e−6/°F	16.53e−6/°F
HMS/Borosilicate (CMC)		
α_l	−0.18e−6/°F	−0.181e−6/°F
α_t	2.59e−6/°F	2.46e−6/°F

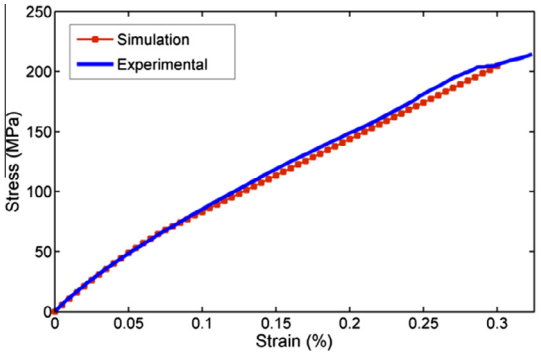

Fig. 8. Nonlinear tensile behavior of plain weave C/SiC.

∼107.5 GPa. Experimental moduli of ∼113.5 and ∼100.0 GPa were obtained by Jacobsen and Brøndsted [12] and Shuler et al. [28] respectively. A subsequent simulation was performed to determine the error that would result if the damage induced during the thermal cool-down of the plain weave CMC was ignored. An initial tensile modulus of 144.8 GPa is predicted for the pristine specimen (i.e., without matrix microcracking), resulting in an overprediction of the as-produced stiffness of the specimen by at least 25%.

Once it was verified that the developed model could accurately predict the as-produced mechanical properties and nonlinear response of a plain weave C/SiC composite, various studies were conducted to investigate in greater detail the damage progression and development of residual stresses. The first study involved modeling a high-fidelity circular fiber using MS-GMC representing a unidirectional composite RUC or a microscale RUC in a woven (e.g., plain weave) composite. Stress free boundary conditions were imposed, and the RUC was subjected to thermal loading (1000 °C reduction in temperature). The matrix constitutive response was governed by the thermoelastic constitutive damage relation, and the fiber was assumed to behave linear elastically. The carbon fiber and silicon carbide matrix material properties were allowed to vary with temperature. Fig. 9 demonstrates the cool-down phase where the mismatch in constituent CTE causes damage initiation and progression due to the development of residual stress. Each contour in Fig. 9 represents the damage state or stress state of the two-dimensional (2D) RUC with a 10% void volume fraction at 200 °C increments over the 1000 °C range. One can recall that the damage variable, λ, begins with a value of one (no damage) and decreases in value, representing the reduction in the load carrying capacity of the matrix material subcell, until it reaches zero. It can be observed that the development of residual stress surrounding the fiber correlates well with the progression of damage. As one would expect, damage initiates first in the cells nearest to the fiber/matrix interface, then progresses outward into the surrounding matrix subcells. Therefore, the degree of damage in a matrix subcell is inversely proportional to its distance from the fiber/matrix interface.

A subsequent study was conducted using a 2D RUC with a high-fidelity circular fiber at the center to investigate the effect of voids on the damage behavior of the ceramic constituent in C/SiC CMCs. The cool-down thermal loading process was simulated for two

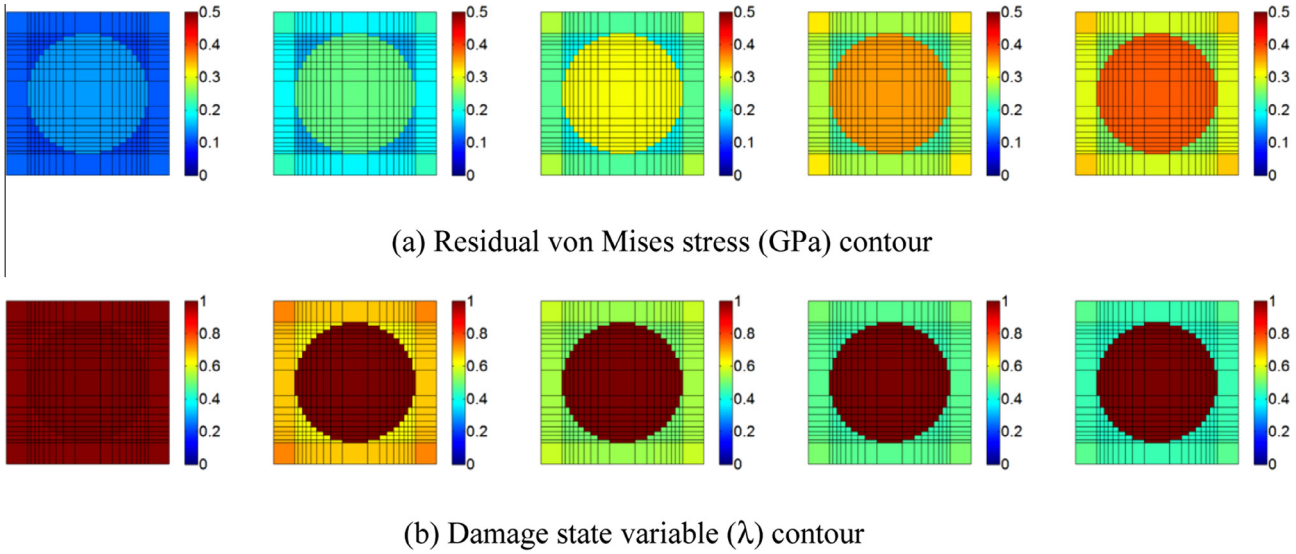

Fig. 9. Residual von Mises stress (GPa) and damage state progression in 2D fiber/matrix subcell RUC during cool-down from 1023 °C to 23 °C.

cases: (i) silicon carbide matrix without voids and (ii) silicon carbide matrix with a 10% volume fraction of intratow voids. Although the tow matrix material of CMCs manufactured using the CVI process will always contain at least a small volume fraction of voids, depending on the manufacturing conditions such as infiltration rate and time, the volume fraction of voids in these composites can vary significantly. Therefore, this study can provide insight into the variation in damage propagation between composites manufactured under conditions that result in varying degrees of porosity. In Fig. 10, damage state variable contours are presented for the two cases. The interphase material was omitted from the contours in Figs. 9 and 10 because it does not significantly contribute to the progressive damage and its presence does not affect the trend in progression of stress and damage within the RUC. Since the progressive damage model is only applied to the matrix material, the damage value/color of the fiber in Fig. 10 remains constant with a value of unity. It can be observed from the contours that damage for the two cases initiates at different temperatures and progresses at varying rates. For example, the contour of the final damage state for the matrix without voids (Fig. 10(a)) shows the presence of greater damage than that of the second case (Fig. 10(b)).

Since it is difficult to gain a quantitative understanding of the damage initiation and progression from the damage variable contours presented in Fig. 10, the multiscale model is called upon to bridge the scales, thereby providing the response at the higher length scales. The phenomenon of matrix damage as a function of porosity is more clearly demonstrated through homogenization of the damage variable over the entire RUC volume to provide an effective damage state of the RUC as shown in Fig. 11. This homogenization, carried out through volume-weighted averaging, is purely for qualitative purpose; the effect of the constituent level progressive damage (i.e., reduction in subcell stiffness) on the higher length scales is accounted for through homogenization of the effective stiffness matrix based on GMC theory [30]. Interestingly, damage initiates earlier in the cool-down process (i.e., at a higher temperature) for the case with matrix voids; however, once the damage initiates in the RUC without matrix

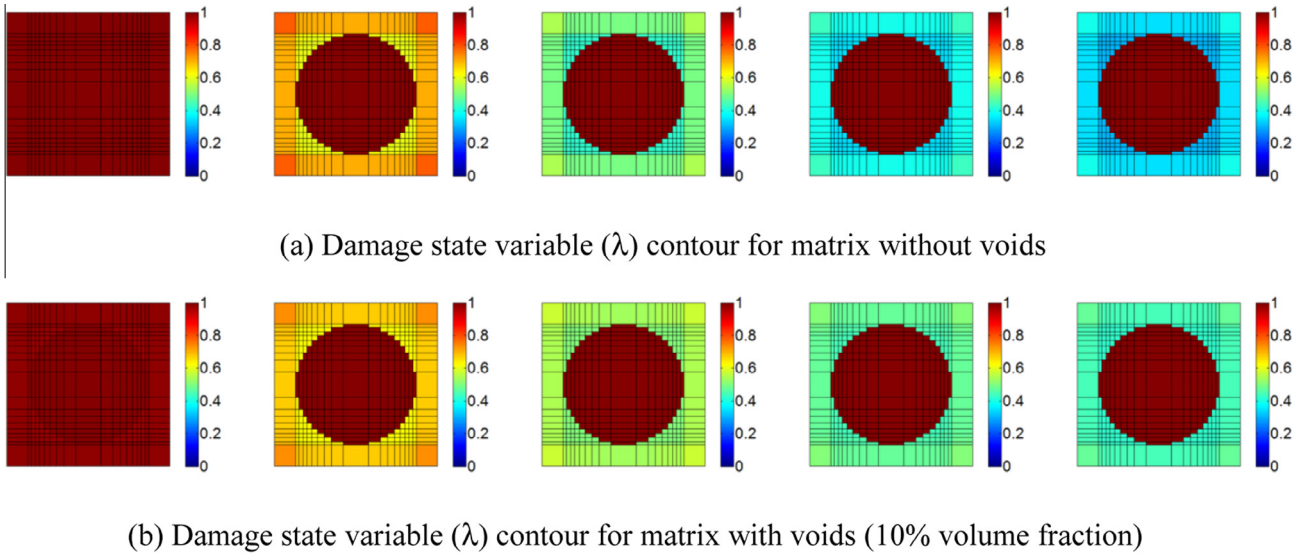

Fig. 10. Damage state progression in 2D fiber/matrix subcell RUC during cool-down from 1023 °C to 23 °C.

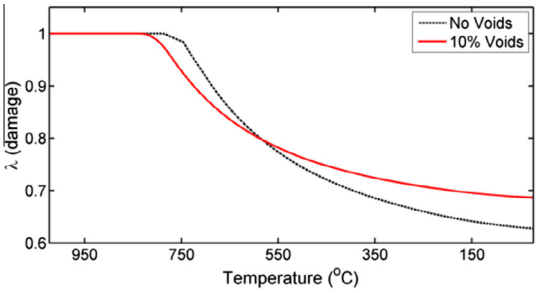

Fig. 11. Effect of matrix voids on damage progression during cool-down in unidirectional C/SiC composite.

voids, the rate of damage is higher and the final reduction in load carrying capacity is greater (i.e., more significant damage). It is hypothesized that the earlier initiation of damage in the matrix with voids is caused by the stress concentration effect of the voids whereas the rapid progression of damage in the matrix without voids is a result of higher concentration of matrix material facilitating more efficient and rapid load transfer between neighboring matrix subcells. Figs. 12 and 13 provide insight into the evolution of elastic moduli (in-plane transverse tensile and shear moduli respectively) as a result of damage over the same range of temperatures. The effect of microscale voids on the initial effective composite tensile and shear moduli can be observed as well as the variation in the reduction of elastic moduli due to matrix damage as a function of temperature.

Moving up the length scales in the multiscale model, the thermoelastic damage behavior of a 2D plain weave C/SiC composite, simulated using a three-dimensional (3D), triply periodic RUC, was investigated during the cool-down phase following the CVI process. By overlaying the plots of the effective damage and tensile modulus vs. temperature, as seen in Fig. 14, it can be observed that the progression of the in-plane tensile modulus, E_{22}, follows that of the damage variable, λ. Recall from Fig. 7 that the elastic moduli of the matrix material increases with a decrease in temperature. Similarly, the effective in-plane modulus of the plain weave composite increases until damage initiates between 700 °C and 600 °C. The undamaged elastic moduli of the matrix material continues to increase as the temperature decreases; however, the increase in the value of the damage variable works to reduce/scale the effective moduli, thereby contributing to the nonlinear behavior. Comparing Figs. 12 and 14, the evolution of the tensile modulus for the plain weave is seen to be more complex. This is due to the increased architectural complexity of the fiber preform (macroscale) and fiber tow bundles (mesoscale), which cause greater heterogeneity in damage and redistribution of stress.

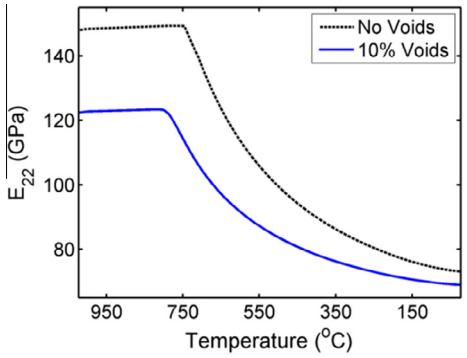

Fig. 12. Effect of matrix voids on tensile modulus reduction during cool-down in unidirectional C/SiC composite.

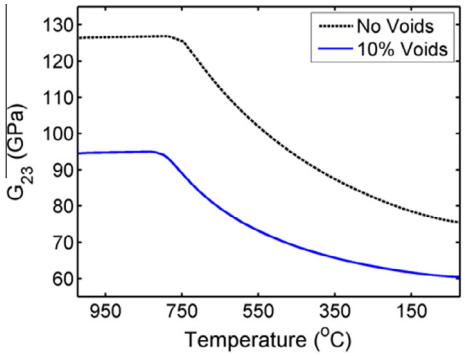

Fig. 13. Effect of matrix voids on in-plane shear modulus reduction during cool-down in unidirectional C/SiC composite.

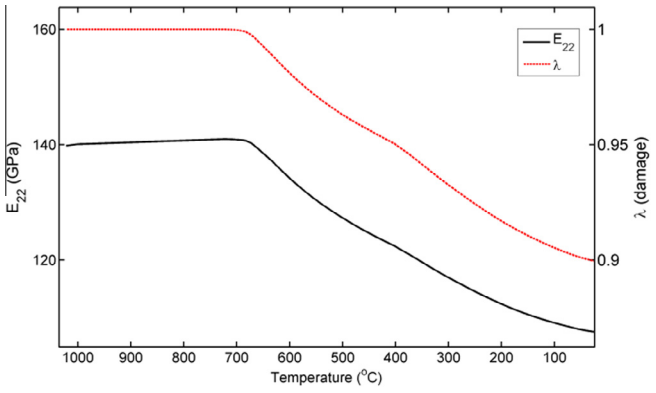

Fig. 14. Damage variable progression and reduction in tensile modulus for plain weave C/SiC composite during cool-down.

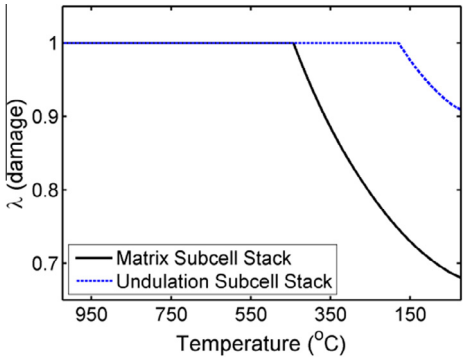

Fig. 15. Damage state variable progression during cool-down for two subcell stacks within the plain weave RUC.

While the homogenized response (elastic and damage) of the 3D RUC during manufacturing and mechanical loading provides insight into the global composite behavior, further investigation can be conducted to obtain information regarding the localized damage behavior in the 3D weave architecture. Therefore, using the multiscale thermoelastic damage framework, the spatial effect within the discretized RUC on damage was determined. A simulation of the manufacturing process of a plain weave C/SiC composite was conducted and the damage as a function of position within various matrix subcells of the RUC presented, as seen in Figs. 15 and 16. Fig. 15 presents a plot of the damage state variable vs. temperature for two matrix subcell stacks. The two subcell stacks, as illustrated in Fig. 17, are composed of matrix cells at the mesoscale.

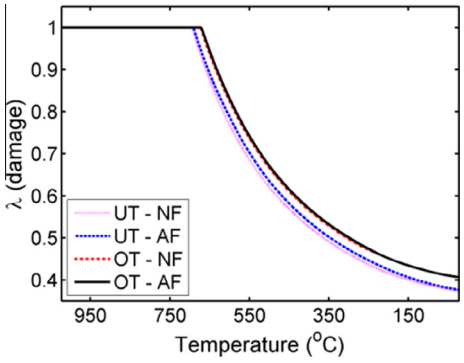

Fig. 16. Damage initiation and progression as a function of position within plain weave RUC.

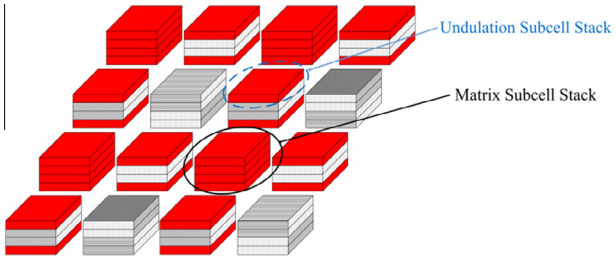

Fig. 17. Matrix subcell stack illustration.

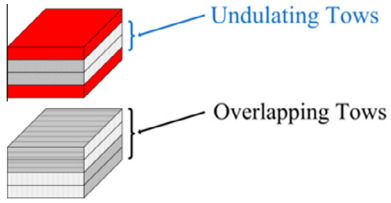

Fig. 18. Tow subcell stack illustration.

Within these matrix subcells, the intertow void content and structure are considered. The 'Matrix Subcell Stack' in Fig. 17 represents a matrix-rich location in the woven RUC caused by the separation of parallel weft and warp fiber tow bundles, while the 'Undulation Subcell Stack' indicates a location at which the undulation of the fiber tow bundle causes high matrix concentration above and below the tow. Through examination of Fig. 15, the difference between the initiation and final state of damage within the two subcells is evident. Damage initiates at a higher temperature and evolves to a greater extent in the homogenized matrix subcell stack as compared with the undulation subcell. This result initially seems counterintuitive since one would expect the presence of fibers in the undulation subcell to cause greater damage as a result of the CTE mismatch. However, after closer inspection of the discretized RUC in Fig. 2, it can be seen that the matrix subcell stack is in contact with fiber subcells (undulating and overlapping) on four sides in addition to at each of the subcell stack corners, as compared to just three sides for the undulating subcell. The increased contact with neighboring fiber tow subcells promotes greater damage within the matrix cells.

Progressing down the length scales to the microscale, the damage initiation and evolution as a function of position within fiber/matrix subcells is investigated and presented in Fig. 16. The damage behavior is examined at two locations within the microscale RUC (near the fiber (NF) and away from the fiber (AF)) for two though-thickness substacks (undulating tow (UT) and overlapping tow (OT)). Illustrations of the through-thickness substacks are presented in Fig. 18, while the microscale RUC used for this analysis is similar to those presented in Fig. 9. From Fig. 16, it is evident that variation in the initiation, progression, and final state of damage exists as a function of RUC location. Therefore, expanded views of the damage initiation and final temperatures are presented in Fig. 19(a) and (b), respectively. Damage is observed initiating at a higher temperature in the cool-down process for the undulating tow cells in comparison with the overlapping tow cells. The damage progresses at similar rates for the two subcell locations while a difference of approximately 8% is present in their final damage states. The earlier initiation and more severe final state of damage for the undulating tows are likely caused by the boundary conditions imposed on the undulating tow by the matrix subcells surrounding it. In other words, the contraction of the matrix subcells will be less than that of the fibers within the undulating tow subcells, therefore subjecting the matrix within the undulating subcells to greater tensile loading. It can also be seen that damage initiates earlier (i.e., at a higher temperature) in matrix subcells near the fiber (NF) compared with those away from the fiber (AF) for both tow subcells investigated. This is in agreement with the results presented in Figs. 9 and 10. As the temperature progresses to room temperature, the damage state variables for the subcell locations near the fiber and away from the fiber appear to converge, indicating damage saturation within the microscale RUC.

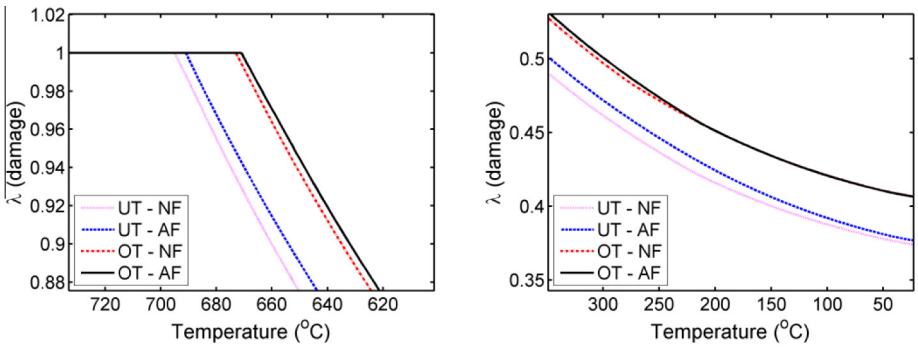

Fig. 19. Expanded views of damage initiation and final state as a function of position within the plain weave RUC.

4. Conclusions

A thermoelastic constitutive damage model is developed and implemented into a multiscale modeling framework to account for the manufacturing-induced residual stresses and strains and resulting matrix microcracking in carbon fiber reinforced CMCs. Capturing the as-produced state of the material system requires consideration of the manufacturing phase following the CVI process. As the composite cools during this phase, microcracks form in the matrix material, causing the as-produced state of the composite to be pre-damaged. The developed thermoelastic matrix damage multiscale framework is able to capture the damage progression during the cool-down phase and accurately models the thermal and mechanical behavior of the composite system. In addition, the initiation and progression of damage and the evolution of effective moduli are studied for different fiber architectures and varying matrix void volume fractions. Overall, the model provides important insights into the thermal, elastic, and damage behavior of carbon fiber reinforced ceramic matrix composites. Future work will include comparison of the simulation results investigating the effect of location on damage behavior with experimental micrographs and tests to further validate the physical accuracy of the developed model. Future work will also address environmental effects (e.g., hot gas infiltration and constituent oxidation) on the mechanical properties of the CMC composite.

Acknowledgments

This work is supported in part by the Army Research Office under Grant No. (60766-EG), Program Manager Dr. Ralph Anthenien; National Science Foundation Graduate Research Fellowship under Grant No. (2011124478); and in collaboration with Aerojet Rocketdyne.

References

[1] Aboudi J. Micromechanical analysis of thermo-inelastic multiphase short-fiber composites. Compos Eng 1995;5(7):839–50.
[2] Aboudi J. The effect of anisotropic damage evolution on the behavior of ductile and brittle matrix composites. Int J Solids Struct 2011;48(14):2102–19.
[3] Aubard X, Lamon J, Allix O. Model of the nonlinear mechanical behavior of 2D SiC–SiC chemical vapor infiltration composites. Am Ceram Soc 1996;77(8):2118–26.
[4] Blackketter DM, Walrath DE, Hansen AC. Modeling damage in a plain weave fabric-reinforced composite material. Compos Technol Res 1993;15(2):136–42.
[5] Bowles D, Tompkins SS. Prediction of coefficients of thermal expansion for unidirectional composites. Compos Mater 1989;23:370–88.
[6] Camus G, Guillaumat L, Baste S. Development of damage in a 2D woven C/SiC composite under mechanical loading: I. Mechanical characterization. Compos Sci Technol 1996;56(12):1363–72.
[7] Dow Chemical Company. CVD SiC Data Sheet. URL: <http://www.dow.com/assets/attachments/business/gt/advanced_ceramics/cvd_silicon_carbide/tds/cvd_silicon_carbide.pdf> [cited 15 March 2013].
[8] El Bouazzaoui R, Baste S, Camus G. Development of damage in a 2D woven C/SiC composite under mechanical loading: II. Ultrasonic characterization. Compos Sci Technol 1996;56(12):1373–82.
[9] Goldberg RK. Utilization of the generalized method of cells to analyze the deformation response of laminated ceramic matrix composites. NASA/TM—217737; 2012.
[10] Hashin Z. Failure criteria for unidirectional fiber composites. Appl Mech 1980;47:329–34.
[11] Inghels E, Lamon J. An approach to the mechanical behaviour of SiC/SiC and C/SiC ceramic matrix composites. Mater Sci 1991;26:5403–10.
[12] Jacobsen TK, Brøndsted P. Mechanical properties of two plain-woven chemical vapor infiltrated silicon carbide-matrix composites. Am Ceram Soc 2001;84(5):1043–51.
[13] Kou WS, Chou TW. Elastic response and effect of transverse cracking in woven fabric brittle matrix composites. Am Ceram Soc 1995;78(3):783–92.
[14] Lamouroux F, Bourrat X, Nasalain R. Structure/oxidation behavior relationship in the carbonaceous constituents of 2D-C/PyC/SiC composites. Carbon 1993;31(8):1273–88.
[15] Lemaitre J, Desmorat R. Engineering damage mechanics: ductile, creep, fatigue and brittle failures. Springer; 2005.
[16] Liu KC, Chattopadhyay A, Bednarcyk B, Arnold SM. Efficient multiscale modeling framework for triaxially braided composites using generalized method of cells. Aerosp Eng 2011;24(2):162–9.
[17] Liu KC, Arnold, SM. Impact of material and architecture model parameters on the failure of woven ceramic matrix composites (CMCs) via the multiscale generalized method of cells, NASA/TM-217011; 2011.
[18] Liu KC, Arnold SM. Influence of scale specific features on the progressive damage of woven ceramic matrix composites (CMCs). CMC 2013;35(1):35–65.
[19] Luo RY, Cheng YH. Effects of preform and pyrolytic carbon structure on thermophysical properties of 2D carbon/carbon composites. Chin J Aeronaut 2004;17(2):112–8.
[20] Mazars J. A description of micro-and macroscale damage of concrete structures. Eng Fract Mech 1986;25(5):729–37.
[21] Mei H, Cheng L, Zhang L, Xu Y. Modeling the effects of thermal and mechanical load cycling on a C/SiC composite in oxygen/argon mixtures. Carbon 2007;45:2195–204.
[22] Murthy PLN, Gyekenyesi JP, Mital SK. Scatter in carbon/silicon carbide (C/SiC) composites quantified; 2004.
[23] Paley M, Aboudi J. Micromechanical analysis of composites by the generalized cells model. Mech Mater 1992;14(2):127–39.
[24] Panchal JH, Kalidindi SR, McDowell DL. Key computational modeling issues in integrated computational materials engineering. Comput Aided Des 2013;45(1):4–25.
[25] Peters PWM, Martin E, Pluvinage P. Influence of porosity and fiber coating on engineering elastic moduli of fiber-reinforced ceramics (SiC/SiC). Am Ceram Soc 1995;78:108–14.
[26] Pradere C, Sauder C. Transverse and longitudinal coefficient of thermal expansion of carbon fibers at high temperatures (300–2500 K). Carbon 2008;46(14):1874–84.
[27] Resende L. A damage mechanics constitutive theory for the inelastic behaviour of concrete. Comput Methods Appl Mech Eng 1987;60(1):57–93.
[28] Shuler SF, Holmes JW, Wu X, Roach D. Influence of loading frequency on the room-temperature fatigue of a carbon-fiber/SiC-matrix composite. Am Ceram Soc 1993;76(9):2327–36.
[29] Sullivan RM, Mital SK, Murthy PLN, Palko JL, Cuneo JC, Koenig JR. Development of design analysis methods for C/SiC composite structures. NASA/TM-214005; 2006.
[30] Aboudi J, Arnold SM, Bednarcyk BA. Micromechanics of composite materials: a generalized multiscale analysis approach. Butterworth-Heinemann; 2012.
[31] Wu JY, Li J, Faria R. An energy release rate-based plastic-damage model for concrete. Int J Solids Struct 2006;43(3):583–612.